Available online www.jsaer.com

Journal of Scientific and Engineering Research, 2020, 7(2):220-229

Research Article

ISSN: 2394-2630
CODEN(USA): JSERBR

Evaluate the Nile River Confluence Morphological Changes on the Shear Layer

Gamal H. El Saeed[1], Neveen A. Badway[2], Hossam M. Elsersawy[3], Fatma S. Ahmed[4]*

[1]Professor of Hydraulics and Water Resources, Faculty of Engineering, Shobra, Benha University, Egypt
[2]Associate Professor, Faculty of Engineering, Shobra, Benha University, Egypt
[3]Associate Professor, Nile Research Institute, National Water Research Center, Egypt
[4]ResearcherAssistant, Nile Research Institute, National Water Research Center, Egypt
*Corresponding Author: fatma_samir2010@yahoo.com

Abstract River channel confluence is one of the morphological features of each river system. It is identified by highly pattern of flow, sediment transport and bed variations. The objectives of this study are: evaluate the Nile River confluence morphological changes on the shear layer, shows the hydraulic and morphological changes at different years, study the nature of sediment transport at channel confluences, its relationship to bed morphology and the variables that control both, comparing contour maps at different years to determine if the sites are changing over time or if the confluent channels remain relatively stable, assessment the effect of the discharge, the momentum flux ratios and angular geometry of confluence in multiple channel systems. The numerical model is applied to simulate the flow pattern and bed topography under wide range of natural conditions. The model was run at three different years 1982, 2003 and 2016. Obtained results illustrate the changes that happened at previous years.

Keywords Confluence, Momentum Flux Ratio, Nile River, Numerical Model and Shear Layer

1. Introduction

The point at which two channels combine marks the site at which large changes must be accommodated in both downstream hydraulic geometry and sedimentary processes. The increase in discharge to which the mainstream must adjust if both channels flood simultaneously has been noted in several studies [16-19-12], whilst the importance of accounting for energy losses within the junction has received attention from [15-8-9].

Research on confluence dynamics is a relatively recent undertaking, and the phenomenon has been studied experimentally in the laboratory, wherein several features have been identified to study the mechanism of flow patterns and bed formation. In studying the hydraulics of a confluence, the plan form angle, discharge ratio, and momentum flux ratio are considered the major controlling factors [3-20]. Several studies [1-17] conducted field investigations of natural stream confluences to assess the relevance of experimental and numerical models for flow composition and morphology under natural conditions. Studies on confluences, including the development of theoretical frameworks, have integrated experimental or field research with numerical modeling [5-14]. A few studies on natural river confluences focused on the combination of flow and sediment transport [11-13-2]. Most experimental and numerical studies on river confluences confirmed that erosion and deposition zones form at the confluence site. The erosion zone involves a morphological process that usually occurs at the beds and outer banks of the river confluence and is known as the scouring hole, which is caused by high velocities. The deposition zone usually occurs at the inner banks (opposite to the location of erosion) and recognized as point bars or islands caused by sediment deposition due to low velocities. Scouring and sedimentation zones are the major morphological features of river confluences. The scour hole is associated with sediment transport caused by increased flow turbulence and velocity intensities at the confluence [6-10-7]. By contrast, deposition can be recognized clearly in the separation zone created under low pressure and flow recirculation. The separation zone in confluences exerts a direct influence on the flow dynamics and morphological features [4-18].

This study selected a River Nile confluence to study. The Nile River has mean features of different shapes of channel confluence such as the confluence downstream islands, connection between side channel and mean river, and the connection of the outlet of the drains and power stations. This study focused at confluence from the islands.

This paper examines the nature of sediment transport at channel confluences, its relationship to bed morphology and the variables that control both. Compare contour maps at different years to determine if the sites are changing over time or if the confluent channels remain relatively stable. Assessment the effect of the discharge, the momentum flux ratios and angular geometry of confluence in multiple channel systems.

2. Materials and Methods

2.1. Study area

An asymmetrical confluence at km 27 from El Roda gauge, near El Marzeek bridge was used for this study. This is an asymmetrical confluence, channelized confluence with a junction angle of 25°, and upstream channel widths (mean (east channel) and tributary (west channel)) of approximately 223 m and 124 m respectively, merging into a downstream channel of width 363 m (figure 1).

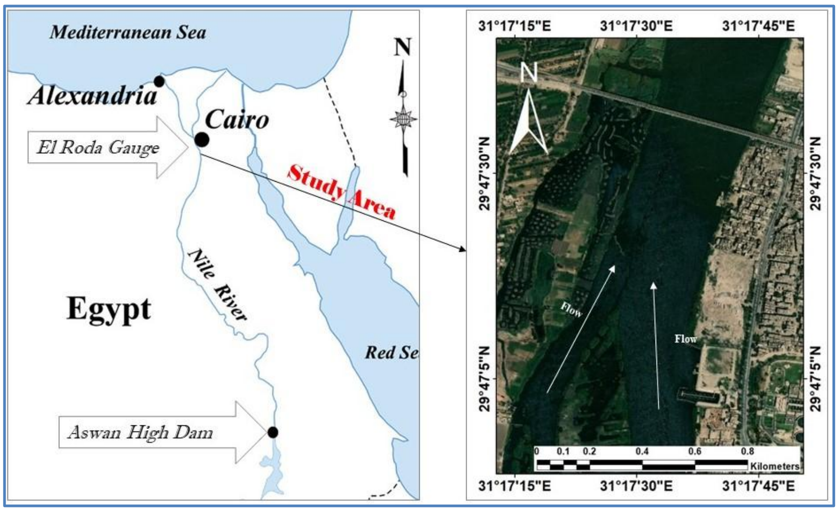

Figure 1: The study confluence and its location

2.2. Methodology

To release the objectives, the following had done:

- Review the literature and collecting the available field data such as bed levels flow velocity, sediment transport, properties of the bed particles and the passing discharge at the selected confluence.
- Collecting the required (bathymetric, hydrological, and hydraulic) data.
- Calibrating the numerical model to make sure it's ability to predict the morphological changed.
- Applying numerical model (Delft) to get the hydraulic properties at the selected confluence at different years.

2.3. Data collection

Large set of data were compiled and used in the analysis which is grouped in two categories. The first category is the data deducted from the historical maps available at Nile Research Institute. These data are the hydrographic maps of Nile River bed produced in 1982, 2003 and 2016. Table 1 shows the geometrical characteristics of the study confluence at the three years.

Table 1: Geometrical characteristics of the study confluence

Years	B_m (m)	B_t (m)	B_{p-c} (m)	ϴ	D_{50} (mm)
1982	241.77	265.04	371.69	37°	0.30
2003	250.48	316.66	363.00	42°	0.40
2016	222.87	123.93	363.00	25°	0.29

Where: B_m= Main channel width, B_t= Tributary channel width, B_{p-c}= the river width downstream of confluence and ϴ= Angle of river confluence.

The second set of data is the hydrological data set presents water level and flow rate downstream Asuit Barrage. The daily monitoring of passing discharges through the located hydraulic structures (barrages) and the upstream and downstream corresponding water levels of those barrages as well as at different gauge stations is essential. Concerning study reach, two-gauge stations El Roda and El Lethyguages are located at Km 0 and Km 53.3 from El-Roda gauge. The water level was collected at El Roda and El LethyGuages as shown in figure 2.

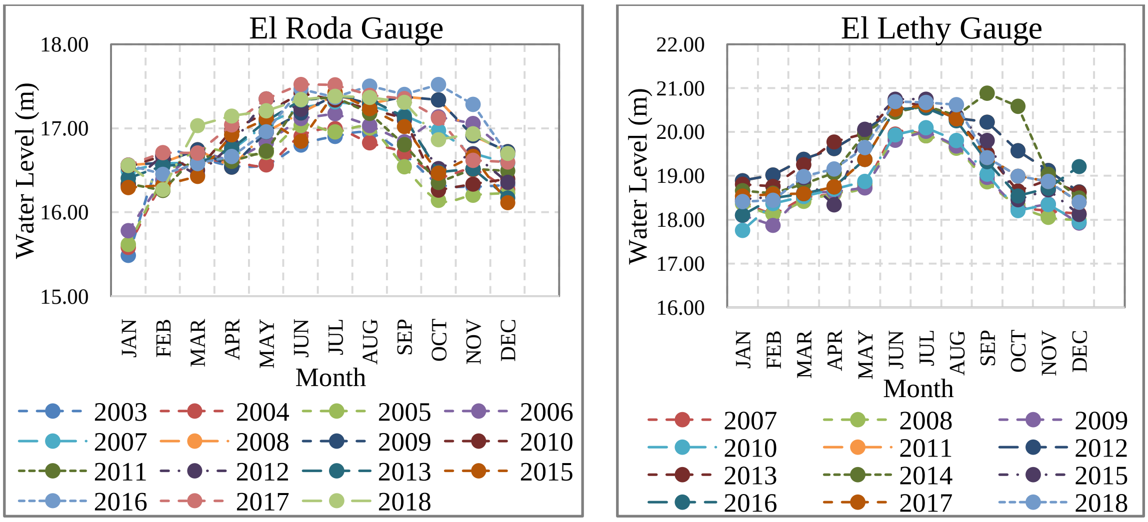

Figure 2: River Nile hydrograph for W.L at El Roda and El Lethygauges

Figure 3 shows the actual average monthly discharges passing D.S. Assiut Barrage during the period from 1982 to 2018, This Figure shows that the maximum discharge is about 182 Mm3/day during the year 2001, while the minimum discharge is 33Mm3/day during year 1997.

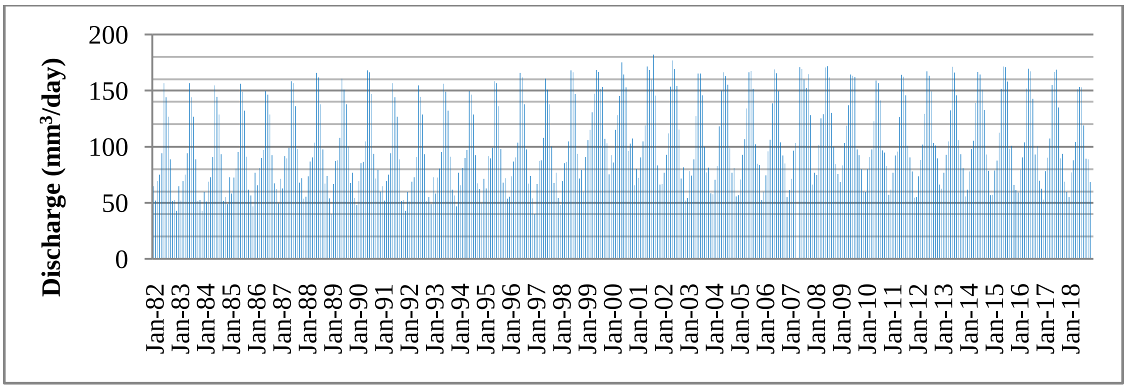

Figure 3: Water Discharge D.S Assuitbarrage from year 1982 to 2018

3. Numerical Model

3.1. Model description

Deltares has developed a unique, fully integrated computer software suite for a multi-disciplinary approach and 3D computations for coastal, river and estuarine areas. It can carry out simulations of flows, sediment transports, waves, water quality, morphological developments and ecology. It has been designed for experts and nonexperts alike. The Delft3D suite is composed of several modules, grouped around a mutual interface, while being capable to interact with one another.

Delft3D-FLOW solves the Navies Stokes equations for an incompressible fluid, under the shallow water and the Boussinesq assumptions. In the vertical momentum equation, the vertical accelerations are neglected, which leads to the hydrostatic pressure equation. In 3D models the vertical velocities are computed from the continuity equation. The set of partial differential equations in combination with an appropriate set of initial and boundary conditions is solved on a finite difference grid, for the numerical aspects. In the horizontal direction Delft3D-FLOW uses orthogonal curvilinear co-ordinates. Two coordinate systems are supported:

- Cartesian co-ordinates ($\xi;\eta$)
- Spherical co-ordinates ($\lambda;\phi$)

The boundaries of a river, an estuary or a coastal sea are in general curved and are not smoothly represented on a rectangular grid. The boundary becomes irregular and may introduce significant discretization errors. To reduce these errors boundary fitted orthogonal curvilinear co-ordinates are used. Curvilinear co-ordinates also allow local grid refinement in areas with large horizontal gradients.

Spherical co-ordinates are a special case of orthogonal curvilinear co-ordinates with:

$$\xi = \lambda, \quad (1)$$

$$\eta = \phi, \quad (2)$$

$$\sqrt{G_{\xi\xi}} = R\cos\phi, \qquad \sqrt{G_{\eta\eta}} = R, \quad (3)$$

In which λ is the longitude, ϕ is the latitude and R is the radius of the Earth (6 378:137 km, WGS84).

3.2. Model construction

Delft 3D model was used to assess morphological changes in the river confluence. The initial input data were imported from a bathymetry survey for the study confluence. A fine unstructured grid (5 m*5 m) consisting of 145587 nodes was created (Figure 4). A finer grid resolution provides more accurate results, but it needs a small-time step (Δt). Time step has a direct relationship with the dimension of the grid and velocity. In the current model, different time steps were attempted until the hydrodynamic simulation operated smoothly with a time step of 0.25s. The second input data comprised the curves of the grain size distribution of the bed material. The measured data indicated that the average median particles of the rivers were approximately 0.3 mm.

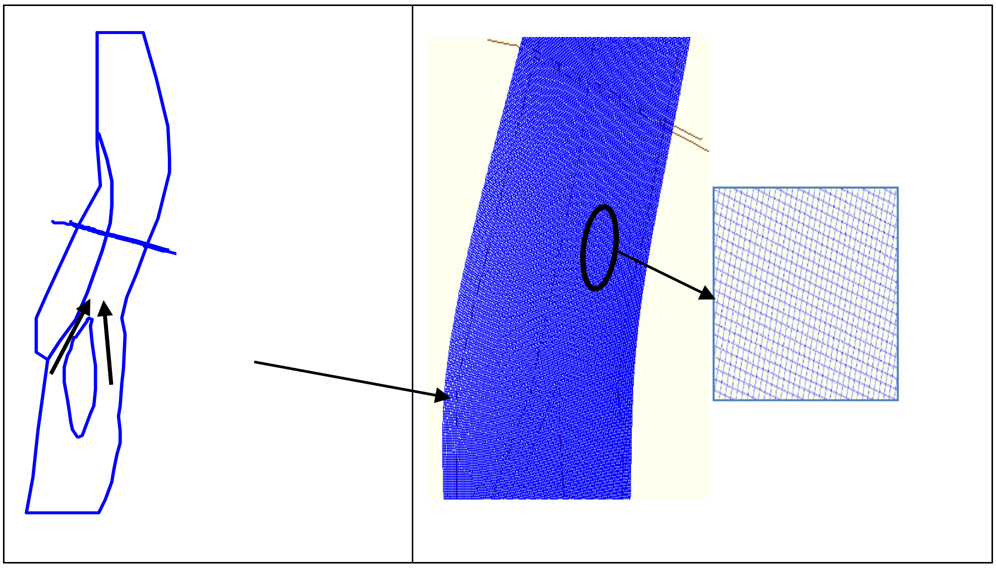

Figure 4: Sample of grid elements composition

3.2. Model calibration

The model was calibrated using the surveyed data at 2003 and the inflow discharges and water levels at different flows as shown in table 2. The location of the cross section showed at figure 5. Comparison of the measured field velocities and obtained velocity profiles at the three cross sections located as shown in figure 5, it showed that there is a good agreement for the calibration.

Table 2: Boundary Condition of the calibration

Calibration Time	Q(m^3/sec)	WL (m)
Jul-2003	1912	18.80
Jan-2011	712	17.46

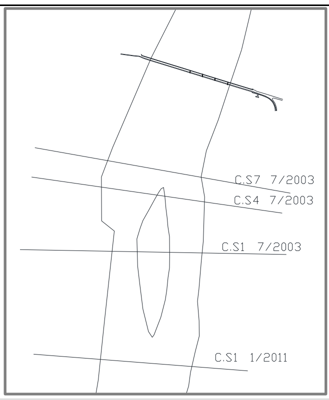

C.S No.	Depth average velocity (m/sec)
C.S 1 (7/2003)	0.87
C.S 2 (7/2003)	0.72
C.S 3 (7/2003)	0.83
C.S (1/2011)	0.37

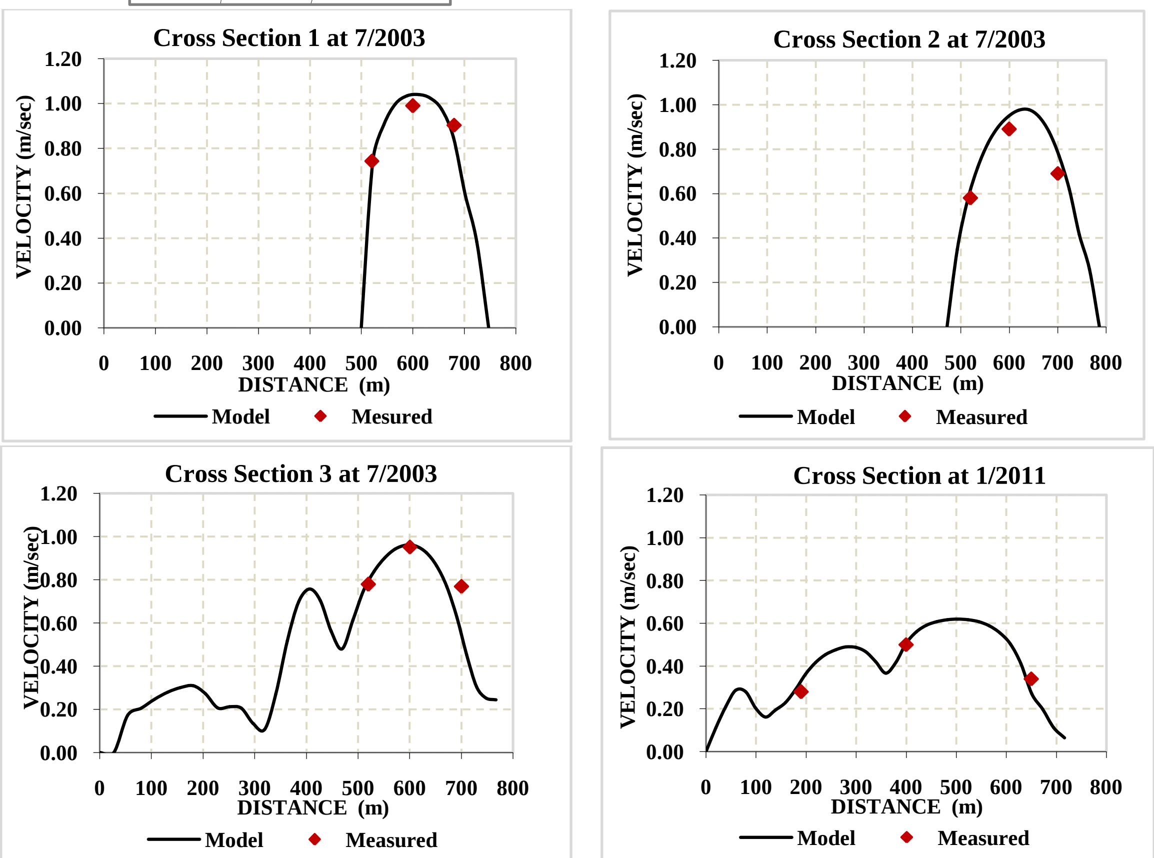

Figure 5: Depth average velocities calibration and the cross sections location

4. Results and Analysis

4.1. Morpho-dynamic at historical years

The reach was simulated at the three years 1982, 2003 and 2016 at different flows (minimum and maximum). Table 3 shows the hydraulic characteristics of the study confluence at max & min flow.

Table 3: Hydraulic characteristics of the study confluence at max & min flow

Years	Q_r		V_r		M_r		F_g		Z (m)
	Max	Min	Max	Min	Max	Min	Max	Min	
1982	1.44	1.15	1.13	0.76	1.62	0.88	0.31	0.15	0.50
2003	0.48	0.20	0.72	0.58	0.35	0.12	0.27	0.11	1.00
2016	0.48	0.12	0.83	0.60	0.40	0.07	0.31	0.14	2.00

Where: Q_r= Discharge ratio, V_r = Velocity ratio, M_r= Momentum flux ratio, F_g= Densimetric Froude number and Z= River bed discordance.

There are several changes at bed elevation occurred at these years as shown at figure 6. The cross sections at figure 7 showed that the bed elevation downstream the confluence completely changes from year 1982 (where the momentum flux ratio was 1.62) to year 2003 and 2016 (where the momentum flux ratio was 0.35 and 0.40 respectively). The location of this cross sections shown in figure 7.

At figure 7 it is noticed that at cross section upstream the confluence the main and tributary channel was eroded at year 2003 and 2016. From cross section 4 to 7 the erosion side was turn from east side (main channel) to the west side (tributary channel). The results have shown that bed morphology at confluences is governed by the junction angle and the ratio between the discharges of the tributary and main channels.

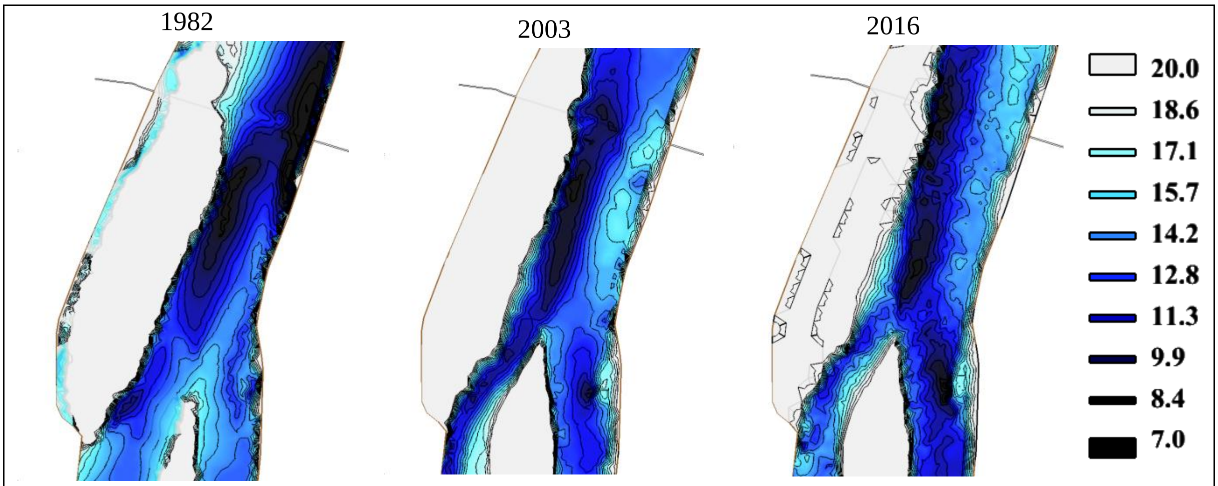

Figure 6: Bed level contours at different years 1982, 2003 and 2016

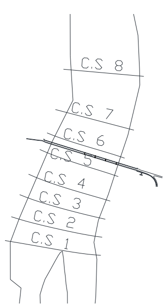

C.S No.	Distance Downstream the Confluence
C.S 1	0
C.S 2	170
C.S 3	340
C.S 4	510
C.S 5	730
C.S 6	890
C.S 7	1120
C.S 8	1505

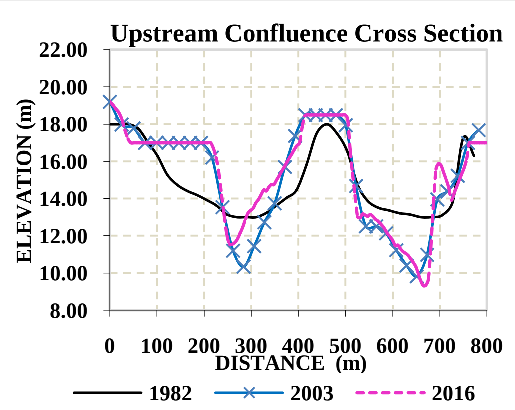

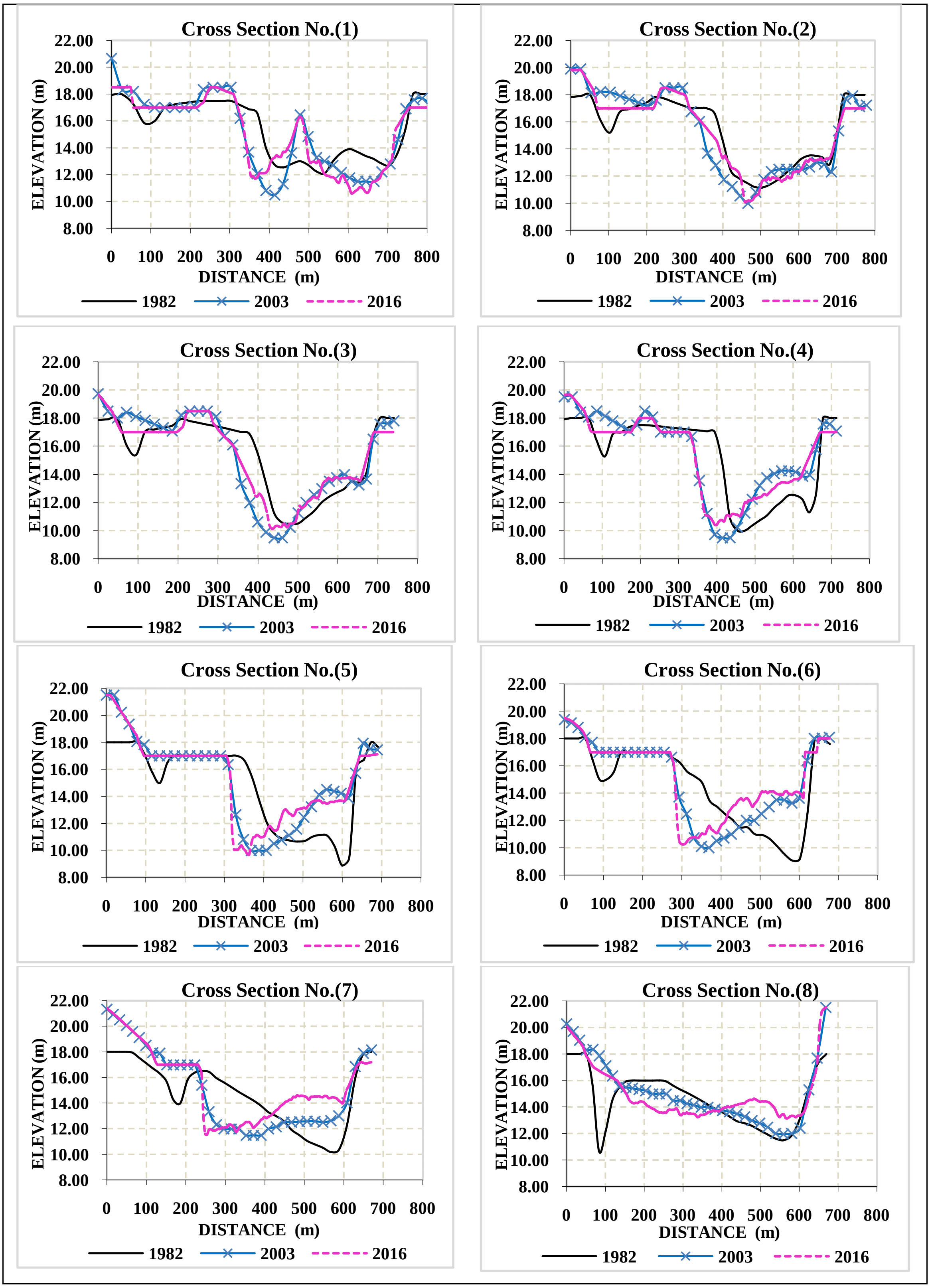

Figure 7: Comparison between the bed elevation at three years 1982, 2003 and 2016

4.2. Hydraulic confluence features results

Figure 8 shows the water surface slope at the location of deepest points at the three years 1982, 2003 and 2016. It's obvious that at year 2016 the slope is higher downstream the confluence than year 2003 and 1982. that mean that the bed elevation at year 2016 was eroded compared with year 2003 and 1982.

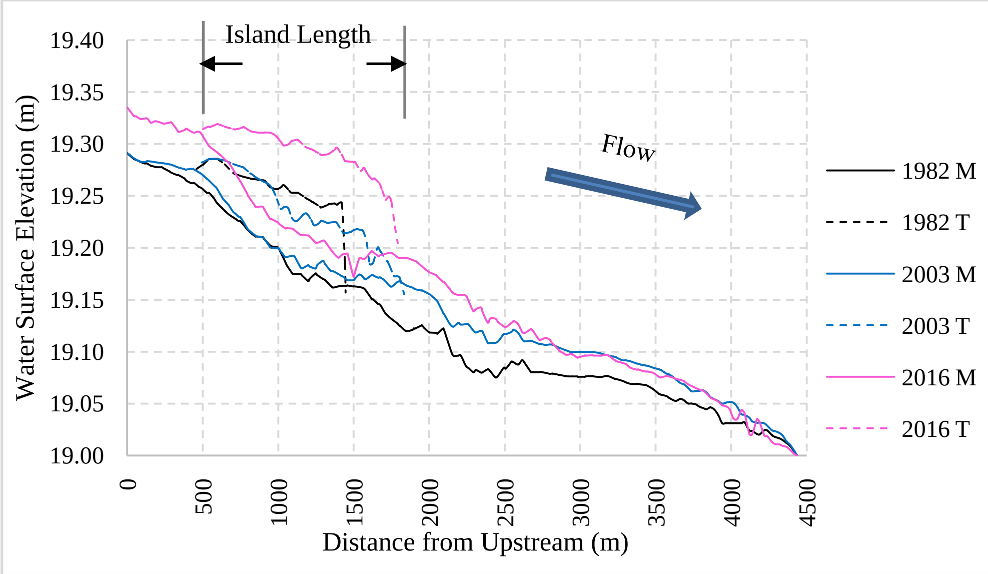

Figure 8: Water surface slope at the deepest points along the reach at the three years in maximum flow, M (main channel) &T (tributary channel)

Figure 9 shows the depth average velocity at maximum flow at the three years 1982, 2003 and 2016. From the figure it is obvious that the velocity at year 1982 has maximum value distributed downstream the confluence along the cross reach, while at year 2003 and 2016 the maximum velocity concentrated toward the main channel. A clear division between high velocity flow from the tributary channel and the highest velocities of the main channel is evident with low intervening velocities marking the shear layer, or mixing interface, between the confluent flows.

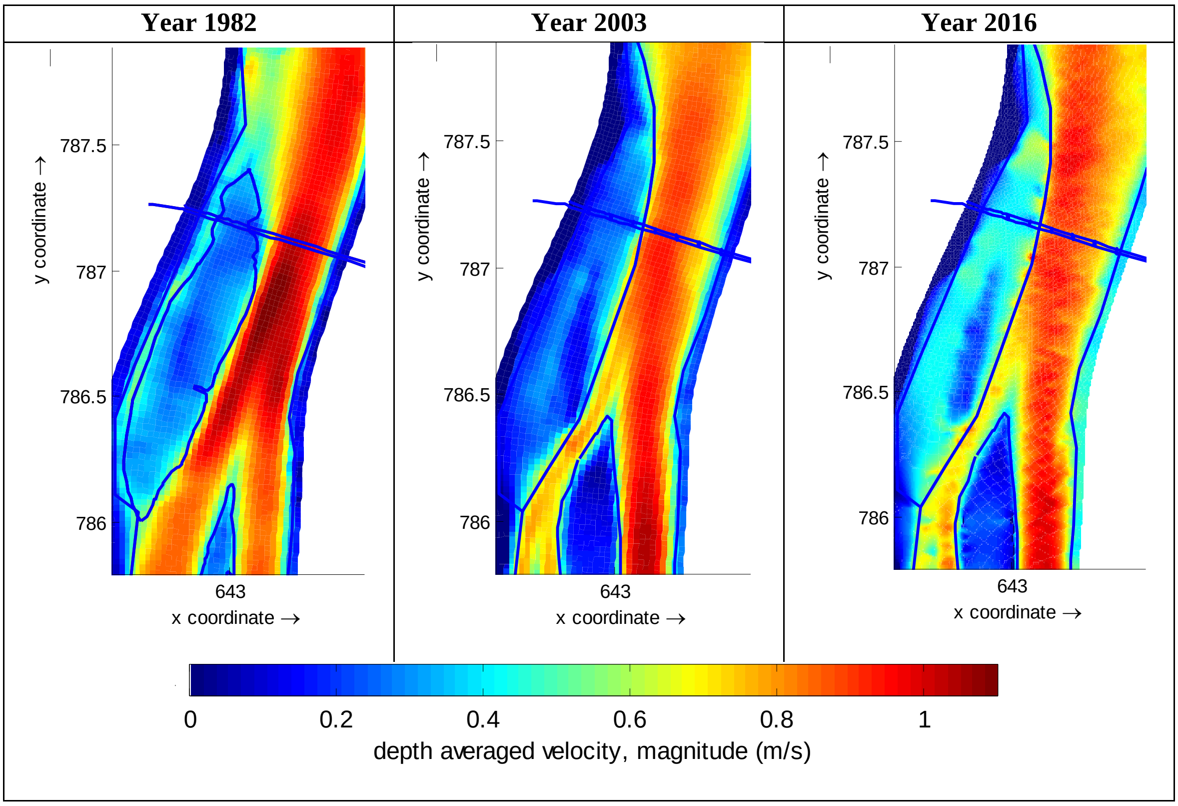

Figure 9: Depth average velocity at maximum flow at the three years

4.3. Mixing shear layer results

Related the sediment transport rates to the variations in momentum flux ratio (*Mr*), which affect to the position of the shear layer and its interaction with the bed morphology. Depending on the distribution of the velocity components, streamlines can be drawn. These streamlines help to discover the discharge ratio between main and tributary channel. Figure 10 shows the streamlines pattern in the confluence channel. As it shows at year 1982 the streamline concentrated at the middle downstream the confluence where $M_r > 1$, while at years 2003 and 2016 it changed towards the west side (tributary channel) where $M_r < 1$. It can help to know the location of the mixing shear layer.

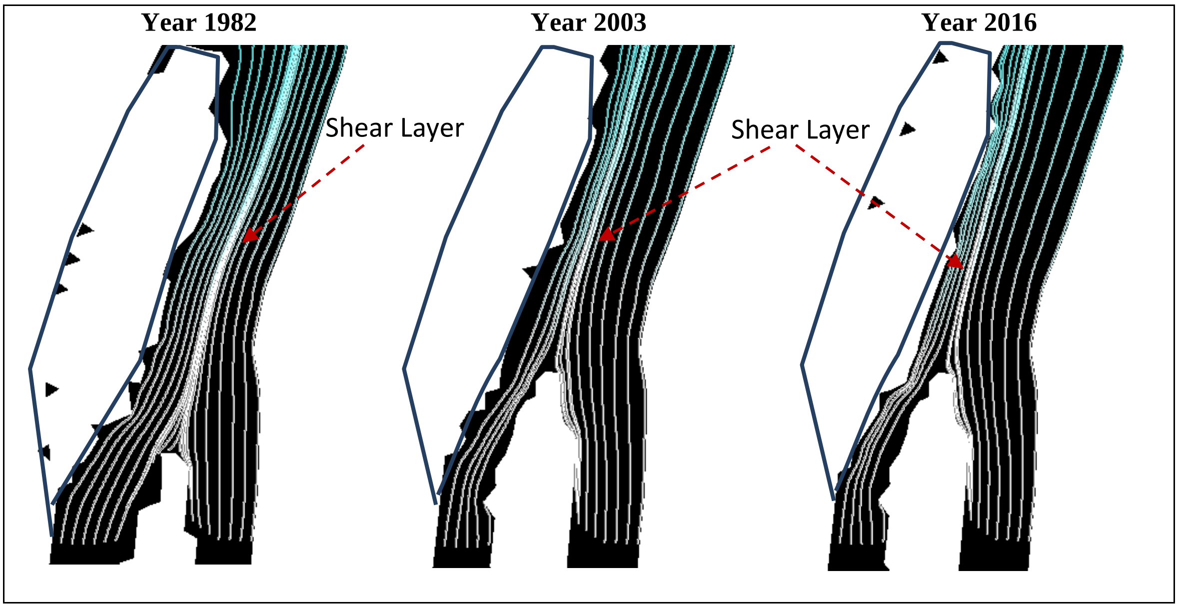

Figure 10: Stream lines at different years

5. Conclusions

The numerical model is applied to simulate the flow pattern and bed topography under wide range of natural conditions. The model was run at three different years 1982, 2003 and 2016. Obtained results illustrate the changes that happed at previous years.

At the studied confluence at year 1982 the streamline concentrated at the middle downstream the confluence where $M_r > 1$, while at years 2003 and 2016 it changed towards the west side (tributary channel) where $M_r < 1$. So, the momentum flux ratio can help to know the location of the mixing shear layer.

The research shows that the distances required for mixing at large river junctions are often long, but can be very short, even within the same junction at different times. The bed morphology at confluences is governed by the junction angle and the ratio between the discharges of the tributary and main channel, which affects the navigation path and the hydraulic structures at the confluence zone.

References

[1]. Ashmore, P.E.; Ferguson, R.I.; Prestegaard, K.L.; Ashworth, P.J.; Paola, C. (1992). Secondary flow in anabranch confluences of a braided, gravel-bed stream. Earth Surf. Process. Landforms, 17, 299–311.

[2]. Ashmore, P.; Gardner, J.T. Unconfined Confluences in Braided Rivers. (2008). In River Confluences, Tributaries and the Fluvial Network; Rice, S., Roy, A., Rhoads, B., Eds.; John Wiley and Sons: Chichester, UK.

[3]. Best, J.L. The Morphology of River Channel Confluences. Prog. Phys. Geogr. (1986). 10, 157–174.

[4]. Birjukova, O.; Guillen, S.; Alegria, F.; Cardoso, A. Three-Dimensional Flow Field at Confluent Fixed-Bed Open Channels. In River Flow.

[5]. Bradbrook, K.F.; Biron, P.M.; Lane, S.N.; Richards, K.S.; Roy, A.G. (1998). Investigation of controls on secondary circulation in a simple confluence geometry using a three-dimensional numerical model. Hydrol. Process, 12, 1371–1396.

[6]. Guillén-Ludeña, S.; Franca, M.J.; Cardoso, A.H.; Schleiss, A.J. (2016). Evolution of the hydromorphodynamics of mountain rivesr confluences for varying discharge ratios and junction angles. Geomorphology, 255, 1–15.

[7]. Leite Ribeiro, M.; Blanckaert, K.; Roy, A.G.; Schleiss, A.J. (2012). Flow and sediment dynamics in channel confluences. J. Geophys. Res. Earth Surf, 117.

[8]. Lin, J.D. and Soong, H.K. (1979). Junction losses in open channel flows. Water Resources Research 15, 414-18.

[9]. Lin, J.D., Scottron, V.E. and Soong, H.K. (1976). Friction effects upon spatially varied open channel flows with increasing discharge. In Rivers ’76, Annual Symposium of the Waterways, Harbours and Coastal Engineering Division of the American Society of Civil Engineers, Fort Collins, Colorado, 10-12 August, 1517-34.

[10]. Rhoads, B.L.; Riley, J.D.; Mayer, D.R. (2009). Geomorphology Response of bed morphology and bed material texture to hydrological conditions at an asymmetrical stream confluence. Geomorphology, 109, 161–173.

[11]. Rice, S.P.; Roy, A.G.; Rhoads, B.L. (2008). River Confluences, Tributaries and the Fluvial Network; JohnWiley& Sons: Chichester, UK. [CrossRef]

[12]. Richards, K.S. (1980). A note on the changes in channel geometry at tributary junctions. Water Resources Research 16, 241-44.

[13]. Riley, J.D.; Rhoads, B.L.; Parsons, D.R.; Johnson, K.K. (2014). Influence of junction angle on three-dimensional flow structure and bed morphology at confluent meander bends during different hydrological conditions. Earth Surf. Process. Landforms, 40, 252–271

[14]. Song, C.G.; Seo, I.W.; Kim, Y. Do. (2012). Analysis of secondary current effect in the modeling of shallow flow in open channels. Adv. Water Resour, 41, 29–48.

[15]. Soong, H.K. (1976). Effect of lateral inflow on steady open channel flows. University of Connecticut, unpublished PhD thesis.

[16]. Stoker, J.J. (1957). Water Waves. New York: Interscience Publishers.

[17]. Szupiany, R.N.; Amsler, M.L.; Parsons, D.R.; Best, J.L. (2009). Morphology, flow structure, and suspended bed sediment transport at two large braid-bar confluences. Water Resour. Res, 45, W05415.

[18]. Thanh, M.; Kimura, I.; Shimizu, Y.; Hosoda, T. (2010). Depth-averaged 2D models with effects of secondary currents for computation of flow at a channel confluence. In Proceedings of the International Conference on Fluvial Hydraulics (River Flow’10), Braunschweig, Germany, 8–10 September; pp. 137–144.

[19]. Thomes, J.B. (1976). Semi-arid erosional systems: case studies from Spain. London School Economics Political Science Geographical Papers 7. 1977: Channel changes in ephemeral streams: observations, problems and models. In Gregory, K.J., editor, River channel changes, Chichester: John Wiley, 317-35.

[20]. Yuan, S.; Tang, H.; Xiao, Y.; Qiu, X.; Zhang, H.; Yu, D. (2016). Turbulent flow structure at a 90-degree open channel confluence: Accounting for the distortion of the shear layer. J. Hydro-Environ. Res, 12, 130–147.